The Future of Data Storytelling for Precipitation Prediction in the Dead- Sea-Jordan Using SARIMA Model

Mohammad Ashraf Ottom[1*], Fayha Al-Shibli[2], Mohammed S. Atoum[3]

[1]*Department of Information Systems, Yarmouk University, Irbid, Jordan; E-mail: ottom.ma@yu.edu.jo*

[2] *Land, Water and Environment Department, University of Jordan, Amman, Jordan*

[3] *King Abdullah II School of Information Technology, University of Jordan, Amman, Jordan*

Abstracts: This research presents a comprehensive study focused on precipitation prediction for the Dead Sea region utilizing the Seasonal Autoregressive Integrated Moving Average (SARIMA) model. The investigation seeks to interpret the accuracy and reliability of the SARIMA model's predictions by comparing them with predictions derived from climate modeling techniques. The evaluation is based on key performance metrics, including Mean Squared Error (MSE), Mean Absolute Error (MAE), and Root Mean Squared Error (RMSE). Additionally, the paper examines the SARIMA model's predictive capabilities through a comparison with actual observations spanning the period from 2010 to 2022. The obtained results reveal an MSE of 12.84593, an MAE of 2.34407, and an RMSE of 3.584123 for this period. Significantly, the SARIMA model surpasses the predictions of prominent climate models (CMIP6), namely ACCESS_CM2, Earth3_Veg, GISS_E2, and HadGEM3, based on comparative performance assessments. The findings emphasize the robustness of the SARIMA model in capturing the essence of the observations and predicting precipitation patterns, not only through its superior performance against climate models but also through its alignment with actual observations. This study contributes to a deeper understanding of precipitation prediction in the Dead Sea region and underscores the potential of the SARIMA model in enhancing forecasting accuracy for hydrological and climatic investigations.

Keywords: Statistical Modeling, Data Science and Climate, Seasonal Autoregressive Integrated Moving Average (SARIMA) Model, Time Series Analysis, Precipitation Prediction, Climate Models, CMIP6-Ssp245

1. INTRODUCTION

The Dead Sea is located in the Jordan Rift Valley at 430 meters (1,410 feet) below sea level, it is the lowest point on Earth's surface, with a salinity of 342 grams per liter, which is roughly ten times saltier than the ocean, additionally, the Dead Sea is also the saltiest body of water on Earth and has a depth of 300 meters, making it the deepest hypersaline lake [1] [2] The Jordan River and a number of other smaller tributaries feed the Dead Sea [3]. The Dead Sea's water level has been dropping for ages, though. The Dead Sea has experienced a slow but worrying decline in water levels over the past few decades; this complicated problem is a result of complex interactions between natural processes, anthropogenic activity, and local water management practices. The Jordan River's declining flow, which has historically been the main supply of water used for recharging the Dead Sea, is at the core of this problem. The building of dams diverted water for industrial and agricultural uses are some of the causes of this drop in river inflow. The hydrological equilibrium of the Dead Sea has been significantly impacted by the resulting decrease in water inflow, which has had a negative impact on the environment and society. The drop of water level in the Dead Sea Lake was estimated to be more than 35% overall during the past thirty years as a result of the water level reduction, which was reported to be occurring at a rate of more than one meter per year [4], [5].

It has become clear that the precipitation pattern in Jordan is inconsistent [6], [7], which calls for careful scientific investigation and thorough research. This drop in rainfall has effects on the hydrological and biological dynamics of the Dead Sea environment because it has been seen over a long period of time. This decrease in rainfall has been attributed to the region's mainly arid and semiarid climate, in addition to larger-scale climatic patterns and shifts. For instance, the mean total precipitation in the Amman Zarqa basin for the years 1971 through 2002 was 215.1 mm, however, the mean total precipitation for the years 2003 through 2016 was statistically lower at 181.3 mm. Fall, winter, and spring combined precipitation decreased from 31.8, 137.6, and 46.1 mm to 24.8, 127.4, and 29.8 mm,

respectively. The patterns of seasonal precipitation distribution between 1971 and 2016 appeared to decline which could have an impact on the dead sea water level [8].

This paper explores the modern difficulties in forecasting rainfall amounts in the Dead Sea basin. The goal of the paper is to offer insights into improving rainfall forecasting accuracy by concentrating on the application of the SARIMA (Seasonal Autoregressive Integrated Moving Average) statistical model. A comparison of SARIMA results with climate models outputs was conducted to investigate its efficiency against the newest ensemble climate projection models CMIP6 under the expected future socio-economic pathway of Jordan in the middle road of challenges ssp245. The rest of the paper is structured as the following: a description of the study area, material and method used in this research, major results and findings, a discussion, and finally a conclusion.

1.1. The Study Area

The study focuses on the precipitation prediction for the Jordanian shores of the dead sea. Figure 1.a shows the study area location in the middle western parts of Jordan. The Figure illustrates surface water basins across Jordan and within the Dead Sea Basin. The basin extends from 31.805ºtop, 31.2225ºbottom, 35.485ºleft and 36.06ºright. Figure 1.b illustrates the digital elevation model of the study area showing the elevation and steep areas below and above sea level in m.

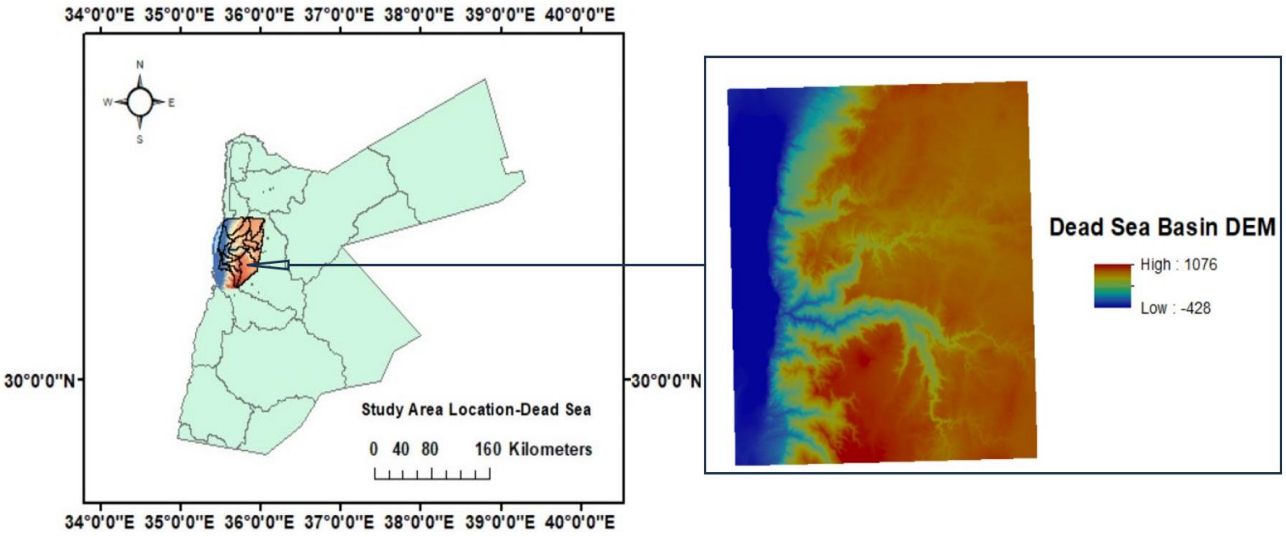

Figure 1: (a) The study location, Dead Sea of Jordan and (b) digital elevation model of the study area

Figure 2.a demonstrates the satellite view of the study area with a river network showing the direction of Wadis and the division of the Dead Sea into two strikingly basins. Figure 2. b shows the land cover and land use classifications within the location of study including Dead Sea water, artificial evaporation bonds in the south, neighbouring dams, urban zones, vegetation cover, and the undeveloped areas indicated bare soils and rocks. Figure 2. c exhibits the isohyets of the Dead Sea basin of average long-term daily rainfall in mm during (1938-2021), the data points (CD0001, CD0003, etc.) are presenting the weather stations for recording the amount of rainfall in mm within the basin and nearby sub-catchments.

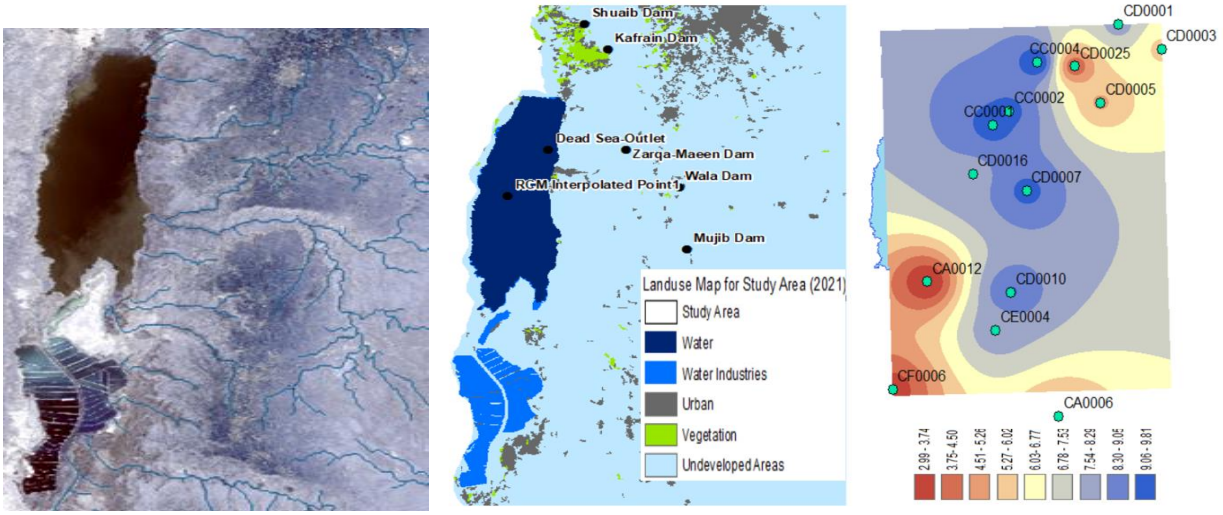

(a) (**b**) **(c)**

Figure 2: (a) satellite view of the study area. (b) land cover and land use classifications. (c) Isohyets of the basin of average long-term daily rainfall (mm) with marked stations ID.

2. MATERIALS AND METHODS

The complexity of the problem at hand is influenced by regional elements such as geological characteristics, climatic variations, and others. The introduction and use of the SARIMA model, a strong statistical method renowned for its efficiency in time-series analysis, is at the heart of this investigation. The chapter digs deep into the workings of the SARIMA model, describing its elements and forecasting approach. The study indicates the model's capability for capturing temporal patterns and fluctuations in rainfall amounts through empirical analysis using actual data. It demonstrates how the SARIMA model may be adjusted to consider the unique features of the Dead Sea basin, providing a tool for more precise and localized precipitation predictions. The chapter also emphasizes the wider effects of accurate rainfall forecasting for the Dead Sea region. Proactive water resource management is made possible by accurate forecasts, which support agricultural planning and infrastructure development.

Time series analysis (TSA) is a statistical and computational technique to examine and evaluate data points gathered over a succession of equally spaced time intervals. The purposes of TSA are to get useful insights, generate predictions, and comprehend variations of historical data, it requires tracking the patterns, trends, and behaviors within a collection across time [9]. In many disciplines, such as economics, finance, environmental science, engineering, and the social sciences, measurements are made at regular intervals, such as hourly, daily, monthly, or yearly. These measurements are known as time series data. By revealing the connections between data elements and their temporal and spatial dependencies, time series analysis enables investigators and analysts to draw conclusions and forecasts based on previously identified trends [10], and ARIMA and SARIMA are considered widely used for analyzing time series data.

SARIMA is the seasonal ARIMA (Autoregressive Integrated Moving Average) which is used to identify patterns and analysis temporal and spatial data. SARIMA was built on top of the ARIMA model, especially when the data show clear seasonal patterns, by adding seasonal elements that accurately represent the cyclical fluctuations present in the time series data. The model is constructed from the following main components: Autoregressive which simulates the association between the current observation and multiple past observations at corresponding seasonal lags, differencing to account for the seasonality (nonstationary), and moving average which combines past forecast errors at seasonal lags to predict the current observation. Equation number 1 represents the SARIMA and the required parameters [11].

$$SARIMA\ (p,d,q) \times (P,D,Q)S \quad (1)$$

where p = AR (Autoregression non-seasonal, d = I (differencing non-seasonal, q = MA (Moving Average non seasonal), P = AR (Autoregression non-seasonal, D = I (differencing seasonal), Q = MA (Moving Average seasonal), S = time length of the seasonal pattern such as daily or monthly, ϕ and θ =non seasonal coefficient value, Φ and Θ = seasonal coefficient value.

AR non-seasonal: $\phi(B) = 1 - \phi_1 B - \cdots - \phi_p B^p$ (2)

MA non-seasonal: $\theta(B) = 1 + \theta_1 B + \cdots + \theta_q B^q$ (3)

Seasonal AR: $\Phi(B^S) = 1 - \Phi_1 B^S - \cdots - \Phi_p B^{PS}$ (4)

Seasonal MA: $\Theta(B^S) = 1 + \Theta_1 B^S + \cdots + \Theta_Q B^{QS}$ (5)

The use of SARIMA model in the field of modeling climate data has been extensively studied, notably for patterns of precipitation. To comprehend and anticipate complicated meteorological occurrences, researchers have taken advantage of SARIMA's capacity to capture seasonal and temporal fluctuations. These studies have shown how well SARIMA captures complex rainfall patterns, which is useful for both short-term forecasting and long-term trend research. The use of SARIMA models is a major methodological strategy in understanding rainfall behavior as climate variability becomes more significant, resulting in improved meteorological insights and informed decision-making. A study by [12] examined the future behavior of monthly average rainfall and temperature in South Asian countries. The study found that climate change has occurred for both rainfall and temperature in these countries and that the SARIMA model can be used to forecast both rainfall and temperature. They utilized climate historical data from January 2011 to December 2021. The study concludes with an understanding of rainfall variation which can be due to climate change. Another study [13] applied the SARIMA model to produce synthetic climate data to be used by hydrological and water resource studies and helps government agencies and policymakers to make the right decisions. Another experimental study [14] isfor predicting future climate parameters such as monsoon rainfall patterns in India (northeast). The study utilized Seasonal Autoregressive Integrated Moving Average (SARIMA) to forecast future precipitation and find the patterns between data. The study has found that the SARIMA ability to predict future rainfall patterns.

Besides SARIMA model, the study elaborated Global Climate Model/Regional Climate Model (GCM/RCM) ensemble Project phase 6 the Coupled Model Intercomparison Project (CMIP6) that provides climate projections to investigate climate change. The ensemble-built diagnosis and evaluation characterized climate datasets[15] based on historical climate forcings of; greenhouse gas and aerosols emissions and concentrations, close-up land use images, clouds circulation, and radiative forcings data from 1850 to 2014. These datasets run the climate models upon their required forcing datasets besides the sensitivity of climate, impacts, and prediction purposes. Different possible scenarios describing the possible future drivers of climate change are included in CMIP6 called shared socio-economic pathways (SSPs). Every pathway suggests a distinctive earth response to force, and the way they explain controllers of climate extremes, available water, and evaluate impacts over land and oceans by conducting different experiments to simulate the future until the year 2100 [16]. The study used four GCM/RCM from the CMIP6 ensemble. Table 1 illustrates the details of each GCM, abbreviation, and the variant used in the study. It is essential to note that ssp245 is the only experiment that has been used here for assessment. The monthly mean precipitation (in mm/day) time series were retrieved from KNMI Explorer by getting the grid point of the Dead Sea (31.27942°N, 35.476586°E) for the period from 1938 to 2050.

The new version of the Australian Community and Earth System Simulator Coupled Model (ACCESS-CM2) model inputs were upgraded by tunning efforts and changes like the diffusion reduction of tropical oceans, heat capacity of seawater, albedo better resolution, and corrected precipitation and canopy evaporation [17]. The Hadley Centre Global Environment Model 3 (HADGEM3) physical climate model was developed to understand the contribution of the mid-warm period to future climate change. This is attributed according to the model point of view to the CO2 level today which is roughly equivalent to CO2 levels in Earth's history and the net loss of energy from the Earth System [18]. The Earth System Model version 3 EC-Earth3 is a promising model that provides an integrated ultra-modern tool for earth system studies. It describes ocean, sea ice, land surface, dynamical vegetation, atmosphere, and its composition. It is characterized by the supplementary data boundary exchange with different earth components [19]. NASA Goddard Institute for Space Studies (GISS) Earth System ModelE2.1 is more conscious of GHG and less warm compared to its version in CMIP5 which is attributed to higher longwave in the simulations which in turn forced climate trends. It also contributes to simulating the drawdown of aquifers for irrigation uses as well as the detection of sea levels [20].

Table 1. Details of each GCM, abbreviation, and variant.

CMIP6 model	Institution	Variant label	Atmospheric lat/lon grid (°)	Forcing	Notes
ACCESS-CM2	CSIRO-ARCCSS Australia	r1i1p1f1	1.25 x 1.87	GHG	Greenhouse gases
				Oz	Troposphere and stratosphere Ozone
				SA	Sulfate aerosols
				SI	Solar irradiance
				VI	Volcanic aerosols
				BC	Black carbon
				OC	Organic carbon
HADGEM 3-GC31-LL	UK Met Office Hadley Center - UK	r1i1p1f3	1.25 x 1.874	All forcing simulation of the recent past	All above forcing including land use change, natural forcing, dust, mineral dust, and sea salt
EC-Earth3-Veg	European Research Consortium EC-Earth -ESM	r3i1p1f1	0.7 x 0.7	GHG Insolation Stratospheric Ozone and aerosols Land use changes	
GISS-E2-1-G-p3	NASA-GISS NASA Goddard Institute for Space Studies USA	r1i1p3f1	2.0 x 2.5	GHG and Aerosols concentration Volcanic and orbital forcings Surface albedo changes and solar irradiance Deforestation	

2.1 The Dataset

The dataset employed for the prediction of future rainfall encompasses a comprehensive compilation of meteorological observations sourced from the Jordan Water Authority (Ministry of Water and Irrigation). Spanning a temporal domain extending from the year 1938 to 2022, this dataset encompasses a substantial chronicle of daily rainfall measurements, quantified in millimeters (mm). The dataset's origin from an authoritative water management entity lends a high degree of credibility to the data's accuracy and reliability. Over this extensive period, the dataset embodies a rich repository of temporal rainfall dynamics, encapsulating both short-term fluctuations and long-term trends. Its inclusion of daily measurements provides a granular perspective, facilitating a good analysis of meteorological patterns at an acceptable temporal resolution. The temporal scope of the dataset encapsulates a holistic view of rainfall behavior within the region over nearly nine decades. This dataset, encouraged by its authoritative source and extensive temporal range, constitutes a robust foundation for the development and validation of predictive models aimed at forecasting future rainfall trends with enhanced precision and contextual insight. Figure 3 shows the rainfall distribution in the study area for the period from 1938 to 2022 (mean daily mm).

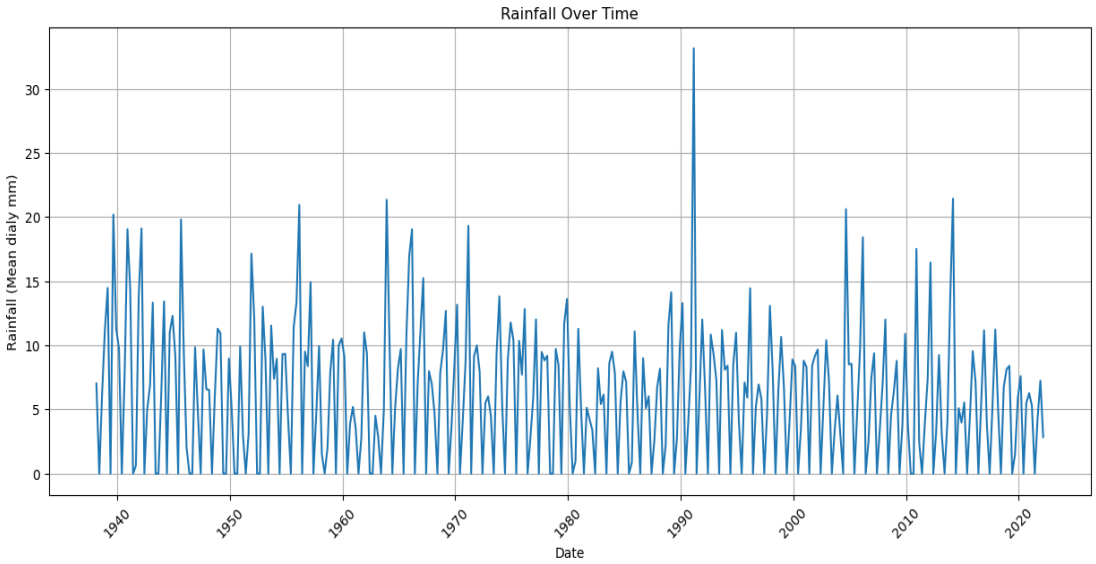

Figure 3: Rainfall over time for the study area for the period from 1938 to 2022 in mean daily mm.

2.2 Preprocessing Phase

The preparation process of the utilized dataset involved a meticulous sequence of procedures to ensure its integrity, consistency, and suitability for subsequent analysis. Initially, the dataset was integrated from two distinct sheets: the first sheet documented daily rainfall measurements spanning from 1938 to 2018, while the second sheet encompassed data from 2019 to 2022. Notably, we addressed the issue of missing values, denoted as -999, by systematically excluding records afflicted by such values. This approach was warranted due to potential sources of missingness, including equipment malfunction or unavailability of data during specific intervals. Furthermore, the date parameter underwent a transformation, converting it into the date and time format to enhance temporal precision.

To capture seasonal variations, the rainfall data was organized into quarters, aligning with meteorological seasons. Specifically, the data was grouped into four quarters: Quarter One (March to May), Quarter Two (June to August), Quarter Three (September to November), and Quarter Four (December to February). Instances, where a quarter lacked recorded data, were treated as instances of zero rainfall, reflecting an assumption that no measurable precipitation occurred during those periods.

For the purpose of model development and evaluation, the dataset was divided temporally into distinct training and testing subsets. The training subset encompassed the interval from 1938 to 2010, providing a substantial historical context for model calibration. On the contrary, the testing subset comprised data from 2011 to 2022, facilitating rigorous model validation against more recent observations. This partitioning ensured that models were rigorously assessed against unseen data, enhancing their generalization and predictive capacity.

The comprehensive preparation process, characterized by data integration, missing value handling, temporal conversion, and seasonal grouping indicated a systemic approach to data preparation. This dataset is prepared to serve as a robust foundation for the development, calibration, and validation of predictive models aimed at forecasting future rainfall trends. The systematic procedurals applied to dataset preparation are integral to the reliability and validity of subsequent analytical activities, affording researchers a robust platform for empirical investigations and informed decision-making in the realm of hydrological and climatic studies.

2.3 Modelling Phase

The training phase of the dataset employed a Seasonal Autoregressive Integrated Moving Average (SARIMA) model, a powerful time series analysis approach widely acknowledged for its ability to capture both temporal and seasonal patterns within data. Given the dataset's yearly nature, an ARIMA model was specifically tailored, with a seasonal parameter denoted as S equal to 12. The training process encompassed iterative model parameter estimation, utilizing historical observations to optimize the model's coefficients and seasonal adjustments. This iterative optimization facilitated the development of a SARIMA model that adeptly accounted for the complex temporal dependencies and seasonal fluctuations present in the dataset. By incorporating both temporal and seasonal components, the SARIMA model determined a holistic understanding of the data's dynamics, thereby enhancing its predictive capabilities. Table 2 shows the results summary for running the model.

Table 2: model summary for ARIMA(1, 1, 1)x(1, 1, 1, 12) with parameters coef (Coefficient), std err (Standard Error), z-score (z), P>|z| (P-value), lower and upper bounds of the 95% confidence

	coef	std err	z	P>|z|	[0.025	0.975]
ar.L1	0.102	0.078	1.309	0.19	-0.051	0.255
ma.L1	-0.9998	2.008	-0.498	0.619	-4.935	2.935
ar.S.L12	-0.1082	0.071	-1.521	0.128	-0.248	0.031
ma.S.L12	-0.8984	0.06	-14.94	0	-1.016	-0.781
sigma2	15.0047	30.002	0.5	0.617	-43.799	73.808

3. RESULTS AND DISCUSSION

By comparing the model's forecasts with testing observations, key performance metrics provide insights into its accuracy and reliability. In this context, the mean squared error (MSE) of 12.8 signifies the average magnitude of squared differences between observed and predicted values. A mean absolute error (MAE) of 2.3 indicates the average absolute discrepancy between the model's forecasts and actual observations. Additionally, the root mean squared error (RMSE) of 3.6 quantifies the square root of the average squared differences, reflecting the model's precision in capturing the variability of daily mean rainfall. These metrics collectively demonstrate SARIMA's proficiency in producing relatively accurate predictions, thereby establishing its viability as a predictive tool for capturing and interpreting intricate rainfall patterns. Figure 4 shows a comparison plot between the model prediction and the corresponding actual (observed) data.

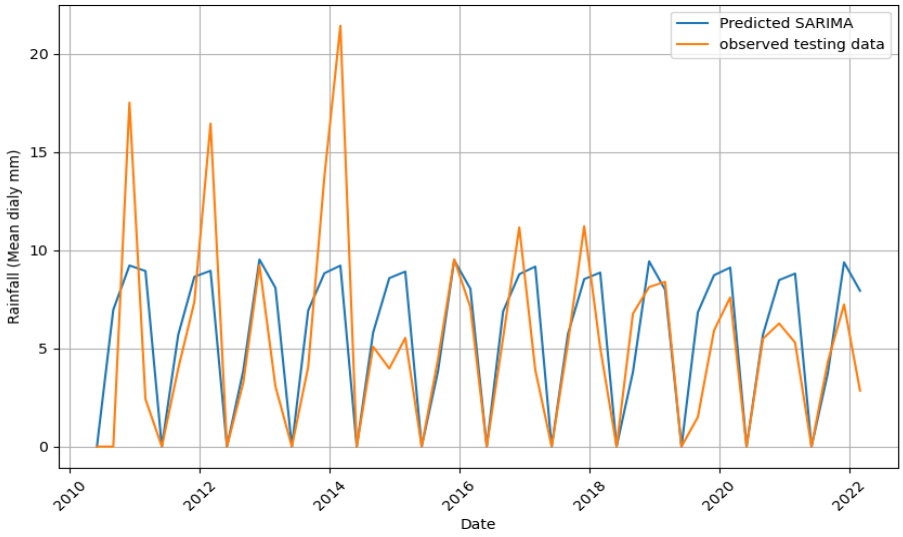

Figure 4: Comparison plot between the model prediction and the corresponding actual (observed) data.

In the pursuit of model validation and performance assessment, a comprehensive comparison was conducted between our approach and the alternative modelling methodologies. Notably, our model exhibited superior performance across key evaluation metrics, including Mean Squared Error (MSE), Mean Absolute Error (MAE), and Root Mean Squared Error (RMSE) as shown in Table 3.

Table 3: Comparison between SARIMA and alternative modelling.

Model	MSE	MAE	RMSE
SARIMA	12.84593	2.34407	3.584123
ACCESS_CM2	22.4615	2.747935	4.739356
Earth3_Veg	38.27498	4.285327	6.186677
GISS_E2	31.68235	3.849951	5.628708
HadGEM3	36.25319	4.194174	6.021062

The evaluation process included a set of validation techniques to ascertain the model's efficiency. In the context of MSE, which quantifies the magnitude of prediction errors, our model consistently yielded lower MSE values in comparison to the alternative models under consideration. Similarly, the MAE assessment indicated that our model achieved reduced absolute prediction errors, signifying its capacity to provide predictions closer to the actual observations. Moreover, the RMSE analysis affirmed our model's superiority by revealing smaller root mean squared errors, thereby attesting to its ability to deliver predictions with diminished overall variance. These consistent trends in performance metrics, across multiple evaluation criteria, highlight the robustness and efficacy of our model as shown in Figure 5.

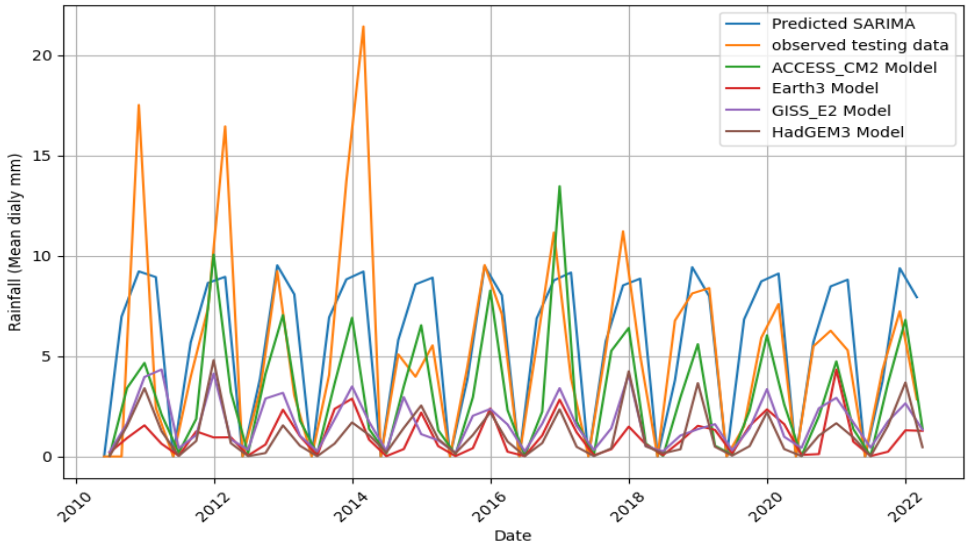

Figure 5: Rainfall prediction comparison between all used models and the observed testing data

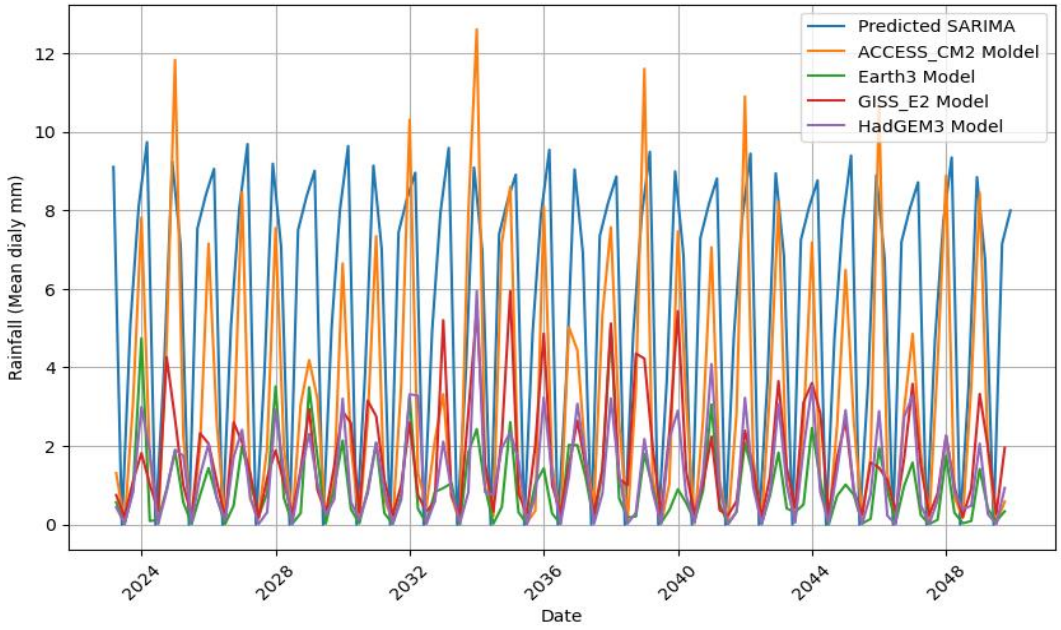

Figure 6: Using the models to predict the amount of rainfall until 2050 for the region of study (the Dead Sea)

In culmination, the conducted study used the models to simulate and predict rainfall patterns with a forward-looking perspective, extending until the year 2050. By employing a rigorous methodological framework that encompassed the utilization of advanced forecasting models as shown in figure 6. The utilization of the models in forecasting rainfall amounts up to 2050 signifies a substantial contribution towards the future hydrological and climatic scenarios, in addition, the rainfall prediction is to inform decision-making and policy formulation to plan ahead and find alternative resources.

The research focuses on evaluating the effectiveness of the SARIMA model in comparison to CMIP6 models for replicating actual observations within a highly vulnerable ecosystem in Jordan. The analysis is conducted under the SSP245 middle-of-the-road scenario, which portrays moderate challenges that the nation must address in the coming years to counteract and adjust to evolving climatic conditions. The primary objective of this study is to demonstrate the accuracy and reliability of SARIMA's predictive capabilities, achieved through a comprehensive

contrast with forecasts generated using climate modelling techniques. The results acquired by the SARIMA model compared to the actual observation demonstrate a Mean Squared Error (MSE) of 12.84593, a Mean Absolute Error (MAE) of 2.34407, and a Root Mean Squared Error (RMSE) of 3.584123 during this specific timeframe (2010-2022).

Notably, the SARIMA model outperforms the forecasts made by well-known climate models (CMIP6). ACCESS-CM2 performed better among the alternative CMIP6 models followed by GISS-E2. HadGEM3 and Earth-CM2 models were slightly aligned simulations of daily precipitations. The GISS-E2 model works more effectively in the spatial distribution of oceanic water and implied energy imbalance leading to warming trends. GISS-E2 model reconsidered water loss in oceans, where the Dead Sea perceived declining surface area due to anthropogenic activities by rerouting its tributaries and changing climate parameters like higher temperature, lower precipitation, and evaporation rates. HadGEM3 is considered one of the warmest models due to its sensitivity to temperature response rather than its hydrological response during the control and simulation periods. Its mean precipitation is around 3.1 mm/day showing less change in precipitation over time (anomaly less than 0.3 mm/day). EC-Earth3-Veg simulated a higher temperature increase by the end of the 21st century because of higher GHG amounts in the atmosphere. So when interpreting this increase to new measures, careful consideration should be taken by continuously recorded GHG concentrations. While GISS-E2 suggested that more energy is transported to deep oceans allowing a smaller rise in atmospheric temperature.

CONCLUSIONS

This study described the prediction of daily precipitation by running SARIMA model and provides a basic assessment for a number of CMIP6 ensemble models' simulations of precipitation during the baseline period and the near future. This study emphasized on the performance of SARIMA against CMIP6 models to simulate real observations in one of the most vulnerable ecosystems in Jordan under the middle road scenario ssp245 which reflects intermediate challenges in the near future that the country should trace for mitigation and adaptation to a changing climate. The research aims to show the precision and dependability of the SARIMA model's predictions by comparing it against projections generated by climate modeling methodologies. The assessment used well-known performance metrics, encompassing Mean Squared Error (MSE), Mean Absolute Error (MAE), and Root Mean Squared Error (RMSE). Furthermore, the study evaluates the predictive ability of the SARIMA model with actual observations spanning the timeframe from 2010 to 2022. The findings disclose an MSE of 12.84593, an MAE of 2.34407, and an RMSE of 3.584123 during this period. Importantly, the SARIMA model demonstrates its dominance over notable climate models—specifically, ACCESS_CM2, Earth3_Veg, GISS_E2, and HadGEM3—based on comprehensive performance evaluations. These results underscore the SARIMA model's robustness in capturing and projecting precipitation trends, not only by outperforming climate models but also by aligning effectively with actual observations. This research enhances the comprehension of precipitation prediction in the Dead Sea region and highlights the SARIMA model's potential to boost forecasting accuracy within hydrological and climatic inquiries.

Data Availability

Data will be available upon request for research purposes.

Conflicts of Interest

The authors declare that there are no conflicts of interest.

REFERENCES

[1]. Al-Halbouni, D.; Alrabayah, O.; Rüpke, L. A Vision on a UNESCO Global Geopark at the Southeastern Dead Sea in Jordan—Geosites and Conceptual Approach. *Land (Basel)* **2022**, *11*, doi:10.3390/land11040549.

[2]. Levy, Y.; Shalev, E.; Burg, A.; Yechieli, Y.; Gvirtzman, H. Three-Dimensional Configuration and Dynamics of the Fresh–Saline Water Interface near Two Saline Lakes with Different Levels (Middle East). *Hydrogeol J* **2021**, *29*, doi:10.1007/s10040-021-02348-6.

[3]. Yechieli, Y.; Reznik, I.J.; Tal, A.; Netzer, L.; Livshitz, Y.; Stein, S. General Information and Hydrogeology of the Mediterranean and Dead Sea Coastal Aquifers and Their Relation with Their Base Level. In; 2021.
[4]. Al-Khlaifat, A.L. Dead Sea Rate of Evaporation. *Am J Appl Sci* **2008**, *5*, doi:10.3844/ajassp.2008.934.942.
[5]. Khlaifat, A.; Batarseh, M.; Nawayseh, K.; Amira, J.; Talafeha, E. Mixing of Dead Sea and Red Sea Waters and Changes in Their Physical Properties. *Heliyon* **2020**, *6*, doi:10.1016/j.heliyon.2020.e05444.
[6]. Freiwan, M.; Kadioğlu, M. Climate Variability in Jordan. *International Journal of Climatology* **2008**, *28*, doi:10.1002/joc.1512.
[7]. Al-Mashagbah, A.; Al-Farajat, M. Assessment of Spatial and Temporal Variability of Rainfall Data Using Kriging, Mann Kendall Test and the Sen?S Slope Estimates in Jordan from 1980 to 2007. *Research Journal of Environmental and Earth Sciences* **2013**, *5*, doi:10.19026/rjees.5.5691.
[8]. Shatanawi, K.; Mohammad, A.H.; Odeh, T.; Arafeh, M.; Halalsheh, M.; Kassab, G. Analysis of Historical Precipitation in Semi-Arid Areas – Case Study of the Amman Zarqa Basin. *Journal of Ecological Engineering* **2022**, *23*, doi:10.12911/22998993/150616.
[9]. Souza, R.C. *Practical Time Series Analysis Prediction with Statistics and Machine Learning*; 2001; Vol. 21;.
[10]. Chatfield, C.; Xing, H. *The Analysis of Time Series: An Introduction with R, Seventh Edition*; 2019;
[11]. Department of Statistics, P.S.U. Applied Time Series Analysis: STAT 510 Available online: https://online.stat.psu.edu/stat510/ (accessed on 11 August 2023).
[12]. Ray, S.; Das, S.S.; Mishra, P.; Al Khatib, A.M.G. Time Series SARIMA Modelling and Forecasting of Monthly Rainfall and Temperature in the South Asian Countries. *Earth Systems and Environment* **2021**, *5*, doi:10.1007/s41748-021-00205-w.
[13]. Martínez-Acosta, L.; Medrano-Barboza, J.P.; López-Ramos, Á.; López, J.F.R.; López-Lambraño, Á.A. SARIMA Approach to Generating Synthetic Monthly Rainfall in the Sinú River Watershed in Colombia. *Atmosphere (Basel)* **2020**, *11*, doi:10.3390/atmos11060602.
[14]. Narasimha Murthy, K. V.; Saravana, R.; Vijaya Kumar, K. Modeling and Forecasting Rainfall Patterns of Southwest Monsoons in North–East India as a SARIMA Process. *Meteorology and Atmospheric Physics* **2018**, *130*, doi:10.1007/s00703-017-0504-2.
[15]. Eyring, V.; Bony, S.; Meehl, G.A.; Senior, C.A.; Stevens, B.; Stouffer, R.J.; Taylor, K.E. Overview of the Coupled Model Intercomparison Project Phase 6 (CMIP6) Experimental Design and Organization. *Geosci Model Dev* **2016**, *9*, doi:10.5194/gmd-9-1937-2016.
[16]. Collins, M.; Minobe, S.; Barreiro, M.; Bordoni, S.; Kaspi, Y.; Kuwano-Yoshida, A.; Keenlyside, N.; Manzini, E.; O'Reilly, C.H.; Sutton, R.; et al. Challenges and Opportunities for Improved Understanding of Regional Climate Dynamics. *Nat Clim Chang* **2018**, *8*, doi:10.1038/s41558-017-0059-8.
[17]. Bi, D.; Dix, M.; Marsland, S.; O'farrell, S.; Sullivan, A.; Bodman, R.; Law, R.; Harman, I.; Srbinovsky, J.; Rashid, H.A.; et al. Configuration and Spin-up of ACCESS-CM2, the New Generation Australian Community Climate and Earth System Simulator Coupled Model. *Journal of Southern Hemisphere Earth Systems Science* **2020**, *70*, doi:10.1071/ES19040.
[18]. Williams, C.J.R.; Sellar, A.A.; Ren, X.; Haywood, A.M.; Hopcroft, P.; Hunter, S.J.; Roberts, W.H.G.; Smith, R.S.; Stone, E.J.; Tindall, J.C.; et al. Simulation of the Mid-Pliocene Warm Period Using HadGEM3: Experimental Design and Results from Model-Model and Model-Data Comparison. *Climate of the Past* **2021**, *17*, doi:10.5194/cp-17-2139-2021.
[19]. Döscher, R.; Acosta, M.; Alessandri, A.; Anthoni, P.; Arneth, A.; Arsouze, T.; Bergmann, T.; Bernadello, R.; Bousetta, S.; Caron, L.-P.; et al. The EC-Earth3 Earth System Model for the Climate Model Intercomparison Project 6. *Geoscientific Model Development Discussions* **2021**.
[20]. Miller, R.L.; Schmidt, G.A.; Nazarenko, L.S.; Bauer, S.E.; Kelley, M.; Ruedy, R.; Russell, G.L.; Ackerman, A.S.; Aleinov, I.; Bauer, M.; et al. CMIP6 Historical Simulations (1850–2014) With GISS-E2.1. *J Adv Model Earth Syst* **2021**, *13*, doi:10.1029/2019MS002034.

DOI: https://doi.org/10.15379/ijmst.v10i1.2794